

Contribution of Apparent Diffusion Coefficient Histogram Analysis Findings in Differential Diagnosis of Parotid Gland Masses

Yeşim Karagöz¹, Hasan Bulut¹, Özdeş Mahmutoğlu², Direnç Özlem Aksoy¹, Abdullah Soydan Mahmutoğlu¹

¹University of Health Sciences Turkey, İstanbul Training and Research Hospital, Clinic of Radiology, İstanbul, Turkey

²University of Health Sciences Turkey, Şişli Hamidiye Etfal Training and Study Hospital, Clinic of Radiology, İstanbul, Turkey

ABSTRACT

Introduction: In this retrospective study, our purpose was to research the usefulness of apparent diffusion coefficient (ADC) histogram graphics for the preoperative diagnosis of parotid tumors with heterogeneous signal distribution.

Methods: Our patient group included 50 patients with total 52 parotid gland masses who had diffusion-weighted imaging and ADC maps before operation or biopsy, which were archived in our institutional Picture Archiving and Communications System. Free-hand region of interest-based ADC histogram parameters were minimum (ADC min), maximum (ADC max), mean (ADC mean) and standard deviation (SD) (ADC SD). Statistical analyses were performed with the SPSS 17.0 using Kruskal-Wallis, Mann-Whitney U tests, Spearman's rho correlation and receiver operating characteristic (ROC) curve.

Results: ADC min, ADC max and especially the ADC mean were statistically significant in differentiating pleomorphic adenoma (PA) from Warthin tumor (WT). ADC min and ADC max values were also significant in differentiating PA from malignant tumor (MT) ($p < 0.05$). In PA-WT differentiation ADC mean value with 1465.50 cut-off level, sensitivity was 94.1% and specificity was 88.6%. For PA-MT differentiation, ADC min value with 962.00 cut-off level, sensitivity was 82.4% and specificity was 94.3%. Whereas, ADC histogram values for WT-MT differentiation were statistically insignificant ($p > 0.05$).

Conclusion: Our results support the assumption that ADC histogram parameters can help discriminate PA from WT and PA from MTs preoperatively. However, they are unhelpful in the differential diagnosis of malignant masses from WT.

Keywords: Diffusion weighted imaging, histogram analysis, apparent diffusion coefficient

Introduction

Parotid tumors comprise about 3% of head and neck neoplasia. Most of these are finally diagnosed as benign. They are frequently located in the parotid gland (1,2). Within parotid gland tumors there are various benign and malignant pathologic subtypes. Differentiation between not only malignant and benign subtypes but also within the benign tumor group is important to make the right choice of treatment strategy, as in the case of potentially malignant pleomorphic adenoma (3,4).

Ultrasound is a preliminary imaging tool for parotid tumor evaluation. It could also guide aspiration cytology. There are some drawbacks of ultrasound: it is only efficient when tumors are superficially located and applied by an expert sonographer (1,4).

Except few indications like sialolithiasis or bone invasion of deep-located tumors, computed tomography is not frequently used because of the relatively low soft tissue resolution (1,5).

Although contrast-enhanced magnetic resonance imaging (MRI) provides detailed structural information, it may accumulate in cerebral tissues even in patients without renal insufficiency (6,7).

Diffusion-weighted imaging (DWI) besides routine MRI series have been frequently used in parotid gland imaging. DWI is known to provide valuable quantitative information not only about components of tissues but also about the microscopic motion of water molecules (8). Apparent diffusion coefficient (ADC) derived parameters have been used for imaging in various organs to differentiate between benign and malignant lesions successfully. In contrast, there are also a few authors reporting that ADC data cannot be helpful in distinguishing between benign and malignant lesions (7,9-11).

In many studies mean ADC values, alone, have been reported not to be discriminative especially in Warthin and malignant groups. Many studies in the English literature also support current research that there is significant overlap between ADC measurements of these lesions (3,11,12).

Histogram analysis has been accepted as the first step texture analysis. In recent literature, there are many reports about histogram analysis of various tumors proven to be a diagnostic tool (13-19).



Address for Correspondence: Yeşim Karagöz MD, University of Health Sciences Turkey, İstanbul Training and Research Hospital, Clinic of Radiology, İstanbul, Turkey
Phone: +90 532 223 99 01 **E-mail:** yesimkar@yahoo.com **ORCID ID:** orcid.org/0000-0002-1000-8271

Cite this article as: Karagöz Y, Bulut H, Mahmutoğlu Ö, Aksoy DÖ, Mahmutoğlu AS. Contribution of Apparent Diffusion Coefficient Histogram Analysis Findings in Differential Diagnosis of Parotid Gland Masses. İstanbul Med J 2022; 23(4): 285-9.

Received: 21.07.2022

Accepted: 19.10.2022

In this study, our aim was to evaluate the preoperative discriminative ability of ADC histogram values not only between malignant and benign parotid tumors but also within each group.

Methods

Study Population

We retrospectively searched the local Picture Archiving and Communications System archive between January 2015 and December 2018. MR DWI of 50 patients, 17 females and 33 males, with parotid masses were evaluated. In two patients ipsilateral multiple lesions were sampled separately. The age range of patients was between 17 and 90 years; the average age was 57.2 years.

All cases had cytological and/or histological diagnoses after MRI. Insufficient sequences or images with prominent artefacts were excluded from our study.

Ethical approval was obtained from the Local Ethics Committee of University of Health Sciences Turkey, İstanbul Training and Research Hospital (approval number: 2337, date: 22.05.2020).

MRI Protocols

MRI examinations were completed on a 1.5-T Signa Hdx MR unit (GE Medical Systems, Milwaukee, WI). Craniovascular or head coils with 8 channels were used to evaluate the upper head and the neck region. Axial and coronal TSE T1W (TR: 580 ms, TE: 13, NEX: 0.50; 5 mm slice thickness); axial, coronal and sagittal TSE T2W (TR: TSE 5400 ms TE: 99 ms; with 90 degrees flip angle: thickness: 4 mm), axial and coronal STIR (TR: 7260 TE: 65 ms; slice thickness: 4 mm) and postcontrast fat-sat T1W (TR: 880 ms TE: 16 ms; slice thickness: 4 mm) sequences were obtained.

Diffusion Weighted Imaging Protocol

At our institution, DW sequence is part of routine head and neck MR examination due to its contribution to differential diagnosis.

Single-shot spin-echo echo-planar imaging sequence (epiDWI) was performed. Imaging parameters were TR: 6250 ms, TE: 97 ms; flip angle: 90; thickness: 4.0 mm; spacing: 1.5 mm; field of view: 20X20 cm; matrix: 128x128; NEX: 1.00 and two sequences with B values 0 and 1000 s/mm² were obtained, respectively.

Image Processing and Interpretation

DWI data were transferred to Advantage Workstation (AW Volumeshare 7, GE Healthcare, Chicago, IL). ADC maps and histogram graphics were derived from epiDWI sequences by integrated software.

Only the solid components were included in the region of interest (ROIs) using data from the fusion of enhanced axial T1W and axial DW images. Gross unenhancing components (possible cystic or necrotic areas) and the surrounding glandular tissue were excluded while drawing free-hand ROIs (Figure 1-3). Slices with largest transverse dimensions of the solid parts were chosen.

Histogram graphics of these ROIs were evaluated to acquire parameters of min, mean, max and standard deviation (SD).

Statistical Analysis

Frequency analysis results were used to describe the distribution of pathological diagnoses within the groups. Mann-Whitney U test was used for differences between tumor groups.

The diagnostic significance of histogram parameters is shown in receiver operating characteristic (ROC) curve analysis. Spearmans' rho correlation was used for relational analysis for pathological diagnosis within groups. Statistical analysis was conducted using the IBM SPSS® Statistics 17 software within 95% confidence interval.

Results

The distribution of histopathological diagnoses of tumors is shown in Table 1.

In the benign group, 56.4% were diagnosed with Warthin tumor, and 43.6% as pleomorphic adenoma (PA). The distribution and statistical relations of mean histogram values of the study groups are shown in Table 2.

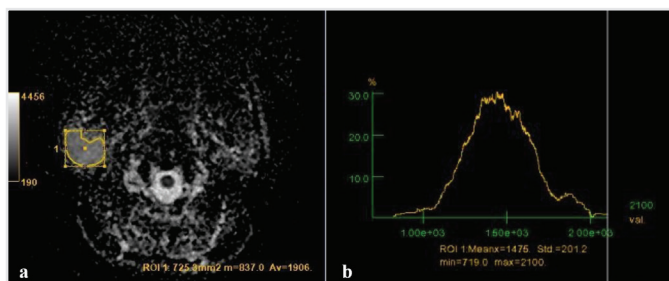


Figure 1. (a, b) Pleomorphic adenomas. Apparent diffusion coefficient maps. ROI with free-hand technique (a) and histogram graphic of the selected ROI (b)
ROI: Region of interest

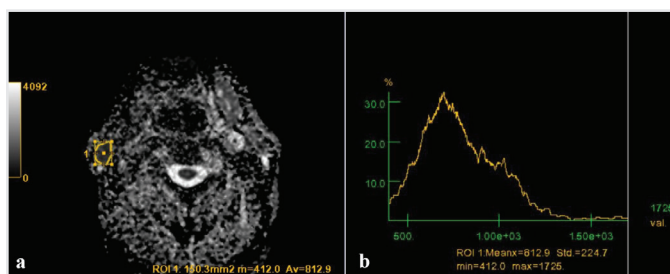


Figure 2. (a, b) Warthin tumor. Apparent diffusion coefficient maps. ROI with free-hand technique (a) and histogram graphic of the selected ROI (b)
ROI: Region of interest

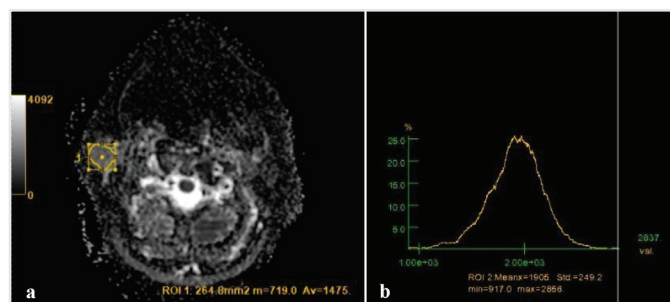


Figure 3. (a, b) Mucoepidermoid cancer. Apparent diffusion coefficient maps. Apparent diffusion coefficient maps. ROI with free-hand technique (a) and histogram graphic of the selected ROI (b)
ROI: Region of interest

All three parameters (ADC min, max and mean) were highest in PAs, while ADC min and mean were the lowest in WTs. The ADC SD parameter was higher in the WTs. Comparisons showed that min, max and mean values were significantly different between the tumor groups ($p < 0.05$). To understand tumor intergroup differences, Mann-Whitney U analysis test was applied (Table 3).

Pair group analysis results showed that SD of ADC did not show a significant difference for any paired group ($p > 0.05$). Additionally, Warthin tumor-malignant tumor differences were statistically insignificant ($p > 0.05$). However, min, max and mean ADC levels were statistically significant for WT-PA and PA-MT pairs ($p < 0.05$). Spearman's rho correlations for malignancy are given in Table 4.

Correlation analysis for malignancy showed that ADC min ($r = -0.728$; $p < 0.001$), max ($r = -0.547$; $p < 0.001$) and mean ($r = -0.776$; $p < 0.001$) values had significant correlations with tumor pairs.

Table 1. Distribution of tumors

	Benign (n=39)	Malignant (n=13)
Warthin tumor	22 (56.4)	-
Pleomorphic adenoma	17 (43.6)	-
Malignant		13 (100.0)

Table 2. Mean values of each histogram parameter (min, mean and max) for each group

	Warthin tumor (n=22)	Pleomorphic adenoma (n=17)	Malignant (n=13)	p
Minimum	430.32±249.98	1148.65±336.47	544.46±319.01	<0.05 ^a
Maximum	1959.91±616.06	2754.94±598.68	1913.08±564.11	<0.05 ^a
Mean	1076.28±342.88	2000.29±336.04	1125.44±377.77	<0.05 ^a
SD	259.69±74.77	242.52±130.04	223.42±99.41	0.260 ^a

^aKruskal-Wallis test, min: Minimum, max: Maximum, SD: Standard deviation

Table 3. Differences within tumor pairs (p-values)

Histogram parameters	Warthin tumor-pleomorphic adenoma	Warthin tumor-malignant	Pleomorphic adenoma-malignant
ADC min	<0.05	0.489	<0.05
ADC max	<0.05	0.960	0.001
ADC mean	<0.05	0.699	<0.05
ADC SD	0.172	0.180	0.967

ADC: Apparent diffusion coefficient, min: Minimum, max: Maximum, SD: Standard deviation

Table 4. Spearman's rho correlation results

Histogram values*	r	p
ADC min	-0.728	<0.001
ADC max	-0.547	<0.001
ADC mean	-0.776	<0.001
ADC SD	-0.005	0.975

*Controlled for malignancy, ADC: Apparent diffusion coefficient, min: Minimum, max: Maximum, SD: Standard deviation

Results of the ROC analysis showed that both ADC min, max and mean levels have diagnostic value for pleomorphic tumor ($p < 0.001$). Area under the curve for ADC min was 0.931, for ADC max was 0.872, and for ADC, mean was 0.965. This shows that ADC min has 93.1%, ADC max has 87.2%, and ADC mean has 96.5% predictive values.

For ADC min with 663.50 cut-off value, sensitivity was 94.1% and specificity was 77.1%. For ADC min with 962.00 cut-off value, sensitivity was 82.4% and specificity was 94.3%.

For ADC max with 2156.50 cut-off value, sensitivity was 94.1% and specificity was 68.6%. For ADC max with 2349.00 cut-off value, sensitivity was 82.4% and specificity was 82.9%.

For ADC mean with 1465.50 cut-off value, sensitivity was 94.1%; specificity was 88.6%. For ADC mean with 1591.50 cut-off value, sensitivity was 88.2% and specificity was 91.4%.

Discussion

Salivary gland tumors are mostly benign involving 54-79% of all. Parotid is the most frequently involved gland. The majority (70-85%) of parotid lesions are also known to be benign (2,18). It is clinically crucial to differentiate between benign and malignant tumors preoperatively because the operator's choice of surgical procedure would change drastically with this information (20). While local excision would be sufficient to excise most benign tumors (with exception of PA), total parotidectomy with or without the sacrifice of the facial nerve would be performed in case of malignancy.

PAs have a high risk of recurrence and malignant transformation. Preoperative diagnosis would change the surgical approach, which will be different to other benign tumors (3,4,9).

Repeated aspiration cytology may be necessary because of insufficient sampling or successful access to deeply located tumor. Therefore, preoperative imaging plays an important role in surgical planning (7,20).

Although there are some clinical findings pointing to malignancy, most parotid tumors grow slowly and the findings such as facial nerve palsy occur late in the disease course (1).

Although sensitivities and specificities are not significant MRI findings of malignant salivary gland tumors include poorly defined borders, low T2W signal intensity, and heterogeneous structure (5,7,8,12,21). Advanced MRI techniques have also been studied for imaging salivary gland tumors. One of the most frequently used additional MRI sequences is DWI (9,19,20,22).

The Yuan et al. (23) also claimed that by adding DWI, MRI would be more powerful diagnostically. In contrast, Eida et al. (19) proposed a multiparametric method using DCE and DW MRI techniques and reported to differentiate benign and malignant tumors. There are other studies suggesting ADC histogram data and time intensity curve derived from gadolinium-enhanced dynamic MR data could be useful for differentiating benign and malignant salivary gland tumors (6,7,24). First-order histogram studies are simple and accessible to many investigators. ADC histogram analysis also appears to be a real advantage for

patients with renal incapacity as it doesn't require intravenous contrast enhancement also considering many recent reports emphasizing intracranial gadolinium deposition (24-26).

Parotid gland tumors have different elements, including tumor cells, lymphoid tissues, myxomatous and necrotic components. Therefore, the analysis of all components of a tumor may cause unreliable results regarding tumor subtyping of tumors (18). Yabuuchi et al. (9) used dynamic enhanced T1W images to choose the tumor section with the lowest ADC value, which enhanced most vividly. Our results were similar to previous report of Habermann et al. (12), using mean ADC values Warthin tumors were found to be distinguishable from PAs and some other benign tumors. They have also failed to reveal any significant differences between WTs and most malignant tumors (12).

There are also some conflicting results in the literature, as in the study of Ma et al. (4), in their study including seventy-three parotid masses they reported that only ADC 10 value was the potential histogram parameter for discriminating malignant and benign tumors.

There are various studies demonstrating the potential of histogram analyses not only for diagnosis but also for grading, differentiating, assessing progression and tumor responses. Higher specificity, sensitivity and accuracy of histogram parameters have often been shown compared with conventional MRI methods or histopathological data (17,18).

In the future, the standardization of histogram data in larger patient populations may be reliable additional tool for MRI to characterize salivary tumors non-invasively.

Study Limitations

The current study was a retrospective study including a small sample size, particularly the number of malignant tumor subtypes. We have included only macroscopically enhancing parts of mass so discarding some parts, which would have added diagnostic value. Studies with larger numbers of both malignant and benign subtypes and with comparisons to whole tumor ROIs would yield more objective results.

Conclusion

Histogram analysis of ADC maps as first line texture analysis appears to provide valuable information about tumor heterogeneity. Although Warthin tumors and malignant lesions could not be differentiated from each other, solely on the basis of histogram values, minimum, mean and maximum ADC histogram parameters are found to be significant to differentiate Warthin tumors from pleomorphic adenomas and pleomorphic adenomas from malignant tumors.

Ethics Committee Approval: Ethical approval was obtained from the Local Ethics Committee of University of Health Sciences Turkey, İstanbul Training and Research Hospital (approval number: 2337, date: 22.05.2020).

Informed Consent: Retrospective study.

Peer-review: Externally peer-reviewed.

Authorship Contributions: Concept: Y.K., Ö.M., A.S.M.; Design: Y.K., Ö.M., A.S.M.; Data Collection or Processing: Y.K., H.B., D.Ö.A.; Analysis or

Interpretation: Y.K., A.S.M.; Literature Search: Y.K., H.B., D.Ö.A.; Writing: Y.K.

Conflict of Interest: No conflict of interest was declared by the authors.

Financial Disclosure: The authors declared that this study received no financial support.

References

- Christe A, Waldherr C, Hallett R, Zbaeren P, Thoeny H. MR imaging of parotid tumors: typical lesion characteristics in MR imaging improve discrimination between benign and malignant disease. *AJNR Am J Neuroradiol* 2011; 32: 1202-7.
- AlKindi M, Ramalingam S, Hakeem LA, AlSheddi MA. Giant Parotid Pleomorphic Adenoma with Atypical Histological Presentation and Long-Term Recurrence-Free Follow-Up after Surgery: A Case Report and Review of the Literature. *Case Rep Dent* 2020; 2020: 8828775.
- Takumi K, Fukukura Y, Hakamada H, Ideue J, Kumagai Y, Yoshiura T. Value of diffusion tensor imaging in differentiating malignant from benign parotid gland tumors. *Eur J Radiol* 2017; 95: 249-56.
- Ma G, Zhu LN, Su GY, Hu H, Qian W, Bu SS, et al. Histogram analysis of apparent diffusion coefficient maps for differentiating malignant from benign parotid gland tumors. *Eur Arch Otorhinolaryngol* 2018; 275: 2151-7.
- Lee YY, Wong KT, King AD, Ahuja AT. Imaging of salivary gland tumours. *Eur J Radiol* 2008; 66: 419-36.
- Kanda T, Fukusato T, Matsuda M, Toyoda K, Oba H, Kotoku JI, et al. Gadolinium-based contrast agent accumulates in the brain even in subjects without severe renal dysfunction: evaluation of autopsy brain specimens with inductively coupled plasma mass spectroscopy. *Radiology* 2015; 276: 228-32.
- Yabuuchi H, Fukuya T, Tajima T, Hachitanda Y, Tomita K, Koga M. Salivary gland tumors: diagnostic value of gadolinium-enhanced dynamic MR imaging with histopathologic correlation. *Radiology* 2003; 226: 345-54.
- Vermoolen MA, Kwee TC, Nivelstein RA. Apparent diffusion coefficient measurements in the differentiation between benign and malignant lesions: a systematic review. *Insights Imaging* 2012; 3: 395-409.
- Yabuuchi H, Matsuo Y, Kamitani T, Setoguchi T, Okafuji T, Soeda H, et al. Parotid gland tumors: can addition of diffusion-weighted MR imaging to dynamic contrast-enhanced MR imaging improve diagnostic accuracy in characterization? *Radiology* 2008; 249: 909-16.
- Celebi I, Mahmutoglu AS, Ucgul A, Ulusay SM, Basak T, Basak M. Quantitative diffusion-weighted magnetic resonance imaging in the evaluation of parotid gland masses: a study with histopathological correlation. *Clin Imaging* 2013; 37: 232-8.
- Matsushima N, Maeda M, Takamura M, Takeda K. Apparent diffusion coefficients of benign and malignant salivary gland tumors. Comparison to histopathological findings. *J Neuroradiol*. 2007; 34: 183-9.
- Habermann CR, Arndt C, Graessner J, Diestel L, Petersen KU, Reitmeier F, et al. Diffusion-weighted echo-planar MR imaging of primary parotid gland tumors: is a prediction of different histologic subtypes possible?. *AJNR Am J Neuroradiol* 2009; 30: 591-6.
- Xu XQ, Hu H, Su GY, Liu H, Hong XN, Shi HB, et al. Utility of histogram analysis of ADC maps for differentiating orbital tumors. *Diagn Interv Radiol* 2016; 22: 161-7.
- Suo S, Zhang K, Cao M, Suo X, Hua J, Geng X, et al. Characterization of breast masses as benign or malignant at 3.0T MRI with whole-lesion histogram analysis of the apparent diffusion coefficient. *J Magn Reson Imaging* 2016; 43: 894-902.
- Zhang Y, Chen J, Liu S, Shi H, Guan W, Ji C, et al. Assessment of histological differentiation in gastric cancers using whole-volume histogram analysis of apparent diffusion coefficient maps. *J Magn Reson Imaging* 2017; 45: 440-9.

16. Xu XQ, Li Y, Hong XN, Wu FY, Shi HB. Radiological indeterminate vestibular schwannoma and meningioma in cerebellopontine angle area: differentiating using whole-tumor histogram analysis of apparent diffusion coefficient. *Int J Neurosci* 2017; 127: 183-90.
17. Schob S, Münch B, Dieckow J, Quäschling U, Hoffmann KT, Richter C, et al. Whole tumor histogram-profiling of diffusion-weighted magnetic resonance images reflects tumorbiological features of primary central nervous system lymphoma. *Transl Oncol* 2018; 11: 504-10.
18. Just N. Improving tumour heterogeneity MRI assessment with histograms. *Br J Cancer* 2014; 111: 2205-13.
19. Eida S, Sumi M, Nakamura T. Multiparametric magnetic resonance imaging for the differentiation between benign and malignant salivary gland tumors. *J Magn Reson Imaging* 2010; 31: 673-9.
20. Papadogeorgakis N, Skouteris CA, Mylonas AI, Angelopoulos AP. Superficial parotidectomy: technical modifications based on tumour characteristics. *J Craniomaxillofac Surg* 2004; 32: 350-3.
21. Swartz JD, Rothman MI, Marlowe FI, Berger AS. MR imaging of parotid mass lesions: attempts at histopathologic differentiation. *J Comput Assist Tomogr* 1989; 13: 789-96.
22. Thoeny HC. Imaging of salivary gland tumours. *Cancer Imaging* 2007; 7: 52-62.
23. Yuan Y, Tang W, Tao X. Parotid gland lesions: separate and combined diagnostic value of conventional MRI, diffusion-weighted imaging and dynamic contrast-enhanced MRI. *Br J Radiol* 2016; 89: 20150912.
24. Ogawa T, Kojima I, Ishii R, Sakamoto M, Murata T, Suzuki T, et al. Clinical utility of dynamic-enhanced MRI in salivary gland tumors: retrospective study and literature review. *Eur Arch Otorhinolaryngol* 2018; 275: 1613-21.
25. Errante Y, Cirimele V, Mallio CA, Di Lazzaro V, Zobel BB, Quattrocchi CC. Progressive increase of T1 signal intensity of the dentate nucleus on unenhanced magnetic resonance images is associated with cumulative doses of intravenously administered gadodiamide in patients with normal renal function, suggesting dechelation. *Invest Radiol* 2014; 49: 685-90.
26. Aime S, Caravan P. Biodistribution of gadolinium-based contrast agents, including gadolinium deposition. *J Magn Reson Imaging* 2009; 30: 1259-67.